

# INTERNATIONAL SOCIETY FOR SOIL MECHANICS AND GEOTECHNICAL ENGINEERING



*This paper was downloaded from the Online Library of the International Society for Soil Mechanics and Geotechnical Engineering (ISSMGE). The library is available here:*

<https://www.issmge.org/publications/online-library>

*This is an open-access database that archives thousands of papers published under the Auspices of the ISSMGE and maintained by the Innovation and Development Committee of ISSMGE.*

# General stress tests on granular materials

## Essais de contrainte générale sur les matériaux granulaires

H.MATSUOKA, Professor, Nagoya Institute of Technology, Nagoya, Japan

Y.SUZUKI, Engineer, Nagoya Port Authority, Nagoya, Japan

T.MURATA, Graduate Student, Nagoya Institute of Technology, Nagoya, Japan

### SYNOPSIS

A general stress apparatus which can apply the general stresses ( $\sigma_x$ ,  $\sigma_y$  and  $\tau_{xy}$ ) directly and independently has been made for a stack of aluminium rods as a two-dimensional model of granular materials. Using this apparatus, "principal stress rotation tests" in which the stress path is the circumference of a Mohr's stress circle are carried out to evaluate the influence of rotation of the principal stress axes on strains, and "general stress path tests" are also performed to investigate the general stress path dependency of strains. These test results are analyzed by the proposed constitutive model by which the general strain increments ( $d\epsilon_x$ ,  $d\epsilon_y$  and  $d\gamma_{xy}$ ) are directly related to the general stress increments ( $d\sigma_x$ ,  $d\sigma_y$  and  $d\tau_{xy}$ ).

### INTRODUCTION

It is natural to consider that the change in stresses on an arbitrary plane causes strains in every kind of material. In the theory of plasticity, however, such an idea is not satisfied because the constitutive relation is usually formulated by the stress invariants such as the principal stresses. For example, the strains caused by the "principal stress rotation test" along a Mohr's stress circle under constant principal stresses cannot be explained by the usual theory of plasticity. Here, using the general stress apparatus, "principal stress rotation tests" and "general stress path tests" are performed, and their test results are analyzed by the proposed model which predicts the strains not only due to "consolidation" and "shear", but also due to "principal stress rotation".

### TWO-DIMENSIONAL GENERAL STRESS APPARATUS

A general stress apparatus which can apply the general stresses ( $\sigma_x$ ,  $\sigma_y$  and  $\tau_{xy}$ ) directly has been made for a stack of aluminium rods (mixture of  $\phi 1.6\text{mm}$  and  $3.0\text{mm}$ ,  $50\text{mm}$  in length) as a two-dimensional model of granular materials. The normal stress  $\sigma_x$  in the vertical direction and the normal stress  $\sigma_y$  in the horizontal direction are applied by the wires connected with air cylinders, and the shear stress  $\tau_{xy}$  is applied by the loading plate on the sample. These three stresses  $\sigma_x$ ,  $\sigma_y$  and  $\tau_{xy}$  can be measured by load cells independently (see Fig.1). The general strains  $\epsilon_x$ ,  $\epsilon_y$  and  $\gamma_{xy}$  can be also measured by dial gauges independently.

### A CONSTITUTIVE MODEL DIRECTLY EXPRESSED IN GENERAL COORDINATES

The following equation has been derived from assuming the hyperbolic relationship between the shear-normal stress ratio ( $\tau_{xy}/\sigma_x$  or  $\tau_{xy}/\sigma_y$ ) and the shear strain ( $\gamma_{xy}$ ) expressed in general coordinates (Matsuoka et al, 1986).

$$\gamma_{xy} = \frac{1}{G_0} \frac{\sin\phi \cdot \sin\phi_{mo} \cdot \sin 2\alpha}{\sin\phi - \sin\phi_{mo}} \quad (1)$$

where  $G_0$  is the gradient of the initial tangent of the hyperbolic relationship,  $\phi$  is the internal friction angle,  $\phi_{mo}$  is the mobilized internal friction angle ( $\sin\phi_{mo} = (\sigma_1 - \sigma_3)/(\sigma_1 + \sigma_3)$ ) and  $\alpha$  is the angle of the principal stress direction. As  $1/G_0 (= k_s)$  is approximately proportional to the logarithm of the mean principal stress  $\sigma_m$ ,  $\gamma_{xy}$  in Eq.(1) is considered to be the function of  $\phi_{mo}$ ,  $\alpha$  and  $\sigma_m$ . By totally differentiating  $\gamma_{xy}$  with respect to  $\phi_{mo}$ ,  $\alpha$  and  $\sigma_m$ , [1] $d\gamma_{xy}^s$ : shear strain increment due to shear ( $d\phi_{mo}$ ), [2] $d\gamma_{xy}^r$ : shear strain increment due to principal stress rotation ( $d\alpha$ ) and [3] $d\gamma_{xy}^c$ : shear strain increment due to anisotropic consolidation ( $d\sigma_m$ ) have been derived as

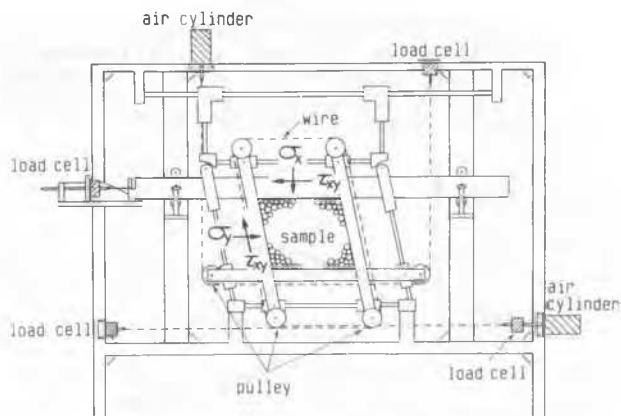


Fig.1 Main Part of Two-dimensional General Stress Apparatus for Rod Mass

follows(Matsuoka et al, 1986):

$$d\gamma_{xy}^s = k_s \cdot \frac{\sin^2 \phi_{mo} \cdot \cos \phi_{mo} \cdot \sin 2\alpha}{(\sin \phi - \sin \phi_{mo})^2} \cdot d\phi_{mo} \quad \text{"shear"} \quad (2)$$

$$d\gamma_{xy}^r = 2k_s \cdot \frac{\sin \phi \cdot \sin \phi_{mo} \cdot \sin 2(\alpha + \delta)}{\sin \phi - \sin \phi_{mo}} \cdot d\alpha \quad \text{"principal stress rotation"} \quad (3)$$

$$d\gamma_{xy}^{ac} = k_c \cdot \frac{\sin \phi \cdot \sin \phi_{mo} \cdot \sin 2\alpha}{\sin \phi - \sin \phi_{mo}} \cdot \frac{d\sigma_m}{\sigma_m} \quad \text{"anisotropic consolidation"} \quad (4)$$

It is considered in  $d\gamma_{xy}^r$ , that the principal stress direction deviates by  $\delta$  from the principal strain increment direction. In order to obtain the normal strain increments  $d\epsilon_x$  and  $d\epsilon_y$  from these shear strain increments, the following stress ratio vs. strain increment ratio relation proposed by Matsuoka(1974) has been introduced.

$$\frac{\tau}{\sigma_N} = \lambda \cdot \left( -\frac{d\epsilon_N}{d\gamma} \right) + \mu \quad (5)$$

where  $\tau/\sigma_N$  is the shear-normal stress ratio on the mobilized plane ( $\tau/\sigma_N = \tan \phi_{mo}$ ),  $d\epsilon_N/d\gamma$  is the normal-shear strain increment ratio on the mobilized plane, and ( $\lambda$  and  $\mu$ ) are the material constants. If Eq.(5) is expressed in general coordinates, we can get the following expression (Matsuoka et al, 1986).

$$\left. \begin{aligned} d\epsilon_x/d\gamma_{xy} \\ d\epsilon_y/d\gamma_{xy} \end{aligned} \right\} = \frac{2 \cdot \frac{\mu - \tan \phi_{mo}}{\lambda} \cdot \cos \phi_{mo} + \sin \phi_{mo} \pm \cos 2\alpha}{2 \cdot \sin 2\alpha} \quad (6)$$

Combining Eqs.(2),(3) and (4) with Eq.(6), the normal strain increments  $d\epsilon_x$  and  $d\epsilon_y$  for these three kinds of shear strain increments can be obtained. It should be noted that  $2\alpha$  in Eq.(6) is changed for  $2(\alpha + \delta)$  when the strains due to "principal stress rotation" are calculated by using Eq.(3). In addition to the above-mentioned strain increments, [4] $d\epsilon_x^{ic} = d\epsilon_y^{ic}$ : normal strain increments due to isotropic consolidation should be taken into account. They are written in a two-dimensional case as follows:

$$\left. \begin{aligned} d\epsilon_x^{ic} \\ d\epsilon_y^{ic} \end{aligned} \right\} = \frac{1}{2} \cdot \frac{0.434C_c}{1 + e_o} \cdot \frac{d\sigma_m}{\sigma_m} \quad \text{or} \quad \frac{1}{2} \cdot \frac{0.434C_s}{1 + e_o} \cdot \frac{d\sigma_m}{\sigma_m} \quad (7)$$

As seen from Eqs.(2)-(7), this constitutive model can predict the strains not only due to "isotropic consolidation", "anisotropic consolidation" and "shear", but also the strains due to "principal stress rotation". As  $d\phi_{mo}$ ,  $d\alpha$  and  $d\sigma_m$  can be expressed by the general stress increments ( $d\sigma_x$ ,  $d\sigma_y$  and  $d\tau_{xy}$ ), the general strain increments can be directly related to the general stress increments as follows :

$$\{d\epsilon_x, d\epsilon_y, d\gamma_{xy}\}^T = [D]^{-1} \cdot \{d\sigma_x, d\sigma_y, d\tau_{xy}\}^T \quad (8)$$

where [D] is the stress-strain matrix.

PRINCIPAL STRESS ROTATION TESTS WITH SEVERAL ROTATION TIMES

Fig.2(a) shows the qualitative pattern of the histogram of the interparticle contact angles expressed in the radial direction, which changes from a circular distribution to an elliptical distribution during shear. Such an elliptical distribution rotates continuously during rotation of the principal stress axes, as shown in Fig.2(b). From  $\alpha=0^\circ$  to  $\alpha=180^\circ$  the elliptical distribution passes in the "virgin" zone in which such structural change has never been experienced, and after  $\alpha=180^\circ$  the experienced structural change will be repeated. Paying attention to the fact that the shear strain increment due to principal stress rotation  $d\gamma_{xy}^r$  has the same parameter  $k_s$  as the shear strain increment due to shear  $d\gamma_{xy}^s$  (see Eqs.(2) and (3) ), the value of  $k_s$  is reduced in the experienced structure by measuring the ratio of the tangential gradient A to B of the cyclic stress-strain relationship at the stress ratio  $\sin \phi_a = 0.25$  which is the same stress ratio as in the principal stress rotation, as shown in Fig.3. This is based on the similarity of the change in structures during cyclic shearing and principal stress rotation (see Fig.2). Fig.4 shows the shear-normal stress ratio vs. normal-shear strain increment ratio relationship on the mobilized plane ( $\alpha = 45^\circ + \phi_{mo}/2$ ) when the stress state circles four times along a Mohr's circle. The broken line in the figure denotes the line of no volumetric strain increment ( $d\epsilon_v = 0$ ). It is seen from Fig.4 that the measured values converge to the line of no volumetric strain increment with the number of rotation times. Therefore, in the analysis the value of the

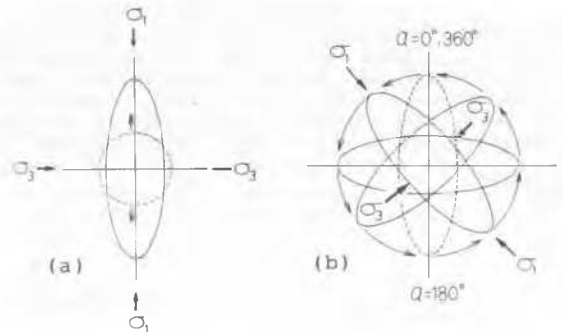


Fig.2 Qualitative Pattern of Histogram of Interparticle Contact Normals Expressed in Radial Direction under (a) Shear and (b) Principal Stress Rotation

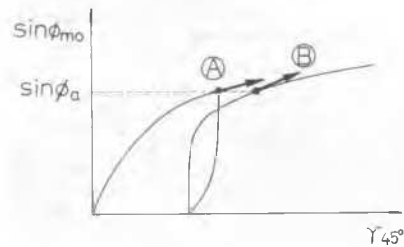


Fig.3 Tangential Gradients of Shear-normal Stress Ratio vs. Shear Strain Relation on 45 Degree Plane under Virgin and Cyclic Loadings

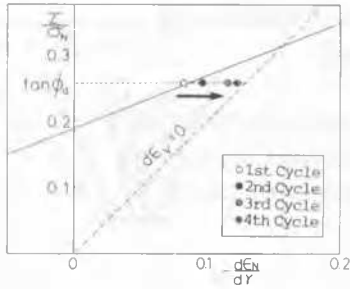


Fig. 4 Shear-normal Stress Ratio vs. Normal-shear Strain Increment Ratio Relation on Mobilized Plane under Four Cycles of Principal Stress Rotation

strain increment ratio is assumed to be the intermediate value between the present value and the value at  $d\epsilon_v = 0$  of the strain increment ratio. Fig.5(a)-(d) shows the results of the principal stress rotation test on the stack of aluminium rods in which the stress state circles four times along a Mohr's circle, and the analytical values by the proposed model. It is seen from this figure that the measured strains in the 2nd to 4th cycles are smaller than in the 1st cycle, and the measured volumetric strain  $\epsilon_v$  becomes smaller with the number of rotation times. The analytical values based on the above-mentioned ideas explains well such tendency of the measured values. In Fig.5(a)-(d) the initial values of strains are taken to be zero.

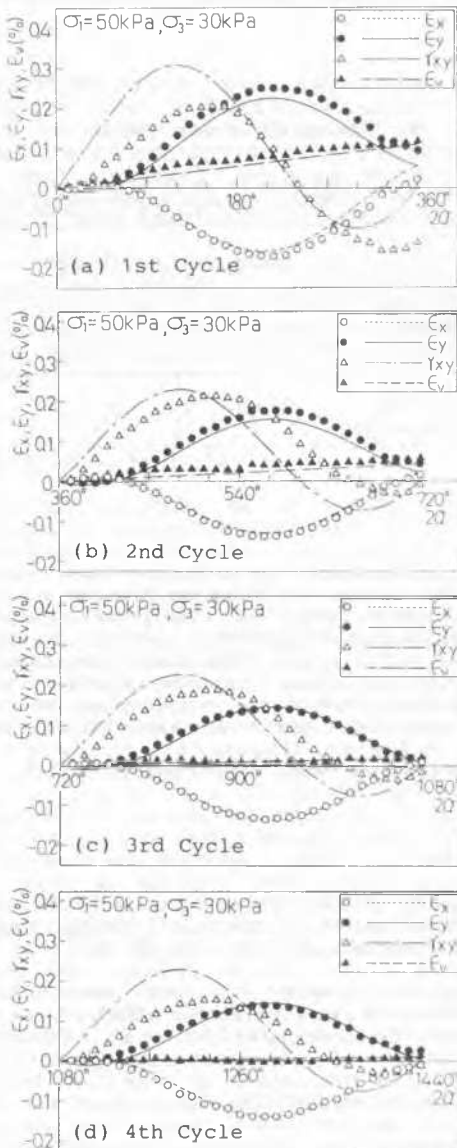


Fig.5 Comparison between Measured and Calculated Strains under Four Cycles of Principal Stress Rotation

THREE KINDS OF "GENERAL" STRESS PATH TESTS

Fig.6 shows three kinds of "general" stress paths ( $A_1 \rightarrow B_1 \rightarrow B_2$ ,  $A_1 \rightarrow B_2$  and  $A_1 \rightarrow A_2 \rightarrow B_2$ ) represented by Mohr's stress circles. TEST ① ( $A_1 \rightarrow B_1 \rightarrow B_2$ ) is the test by which the principal stress rotation ( $B_1 \rightarrow B_2$ ) is induced after shearing ( $A_1 \rightarrow B_1$ ). TEST ② ( $A_1 \rightarrow B_2$ ) is the test by which the principal stress rotation and shearing are induced at the same time. TEST ③ ( $A_1 \rightarrow A_2 \rightarrow B_2$ ) is the test by which shearing ( $A_2 \rightarrow B_2$ ) is induced after the principal stress rotation ( $A_1 \rightarrow A_2$ ). It should be noted that the same starting point  $A_1$  and the same final point  $B_2$  are selected in the three kinds of "general" stress paths, and the principal stress values at  $A_1$  and  $A_2$  are the same ( $\sigma_1 = 45$ ,  $\sigma_3 = 35$  kPa) and the principal stress values at  $B_1$  and  $B_2$  are also the same ( $\sigma_1 = 50$ ,  $\sigma_3 = 30$  kPa). Therefore, the difference of the above three kinds of "general" stress paths cannot be expressed in the  $\sigma_1 \sim \sigma_3$  diagram or the  $q-p$  diagram ( $p = (\sigma_1 + \sigma_2 + \sigma_3)/3$  and  $q = \sigma_1 - \sigma_3$ ). Fig.7(a)-(c) shows the measured values by TEST ①, ② and ③ and the analytical values by the proposed model, represented by the relation between the principal stress ratio ( $\sigma_1/\sigma_3$ ) and strains ( $\epsilon_x, \epsilon_y, \gamma_{xy}, \epsilon_1, \epsilon_3, \epsilon_1 - \epsilon_3, \epsilon_v = \epsilon_1 + \epsilon_3$ ). The parts where  $\sigma_1/\sigma_3$  is constant in Fig.7(a) and (c) correspond to the principal stress rotation under constant principal stresses ( $B_1 \rightarrow B_2$  and  $A_1 \rightarrow A_2$  in Fig.6). In Fig.7(a), the final calculated values of these strains are indicated by arrows. Fig.7(b) corresponds to the case when the increase in the principal stress ratio (i.e., shearing) and the rotation of the principal stress axes occur at the same

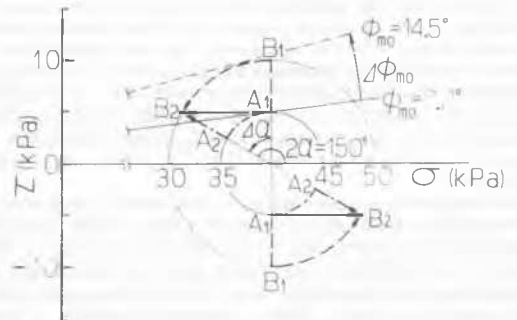


Fig.6 Three Kinds of "General" Stress Paths ( $A_1 \rightarrow B_1 \rightarrow B_2$ ,  $A_1 \rightarrow B_2$  and  $A_1 \rightarrow A_2 \rightarrow B_2$ ) by Mohr's Stress Circles

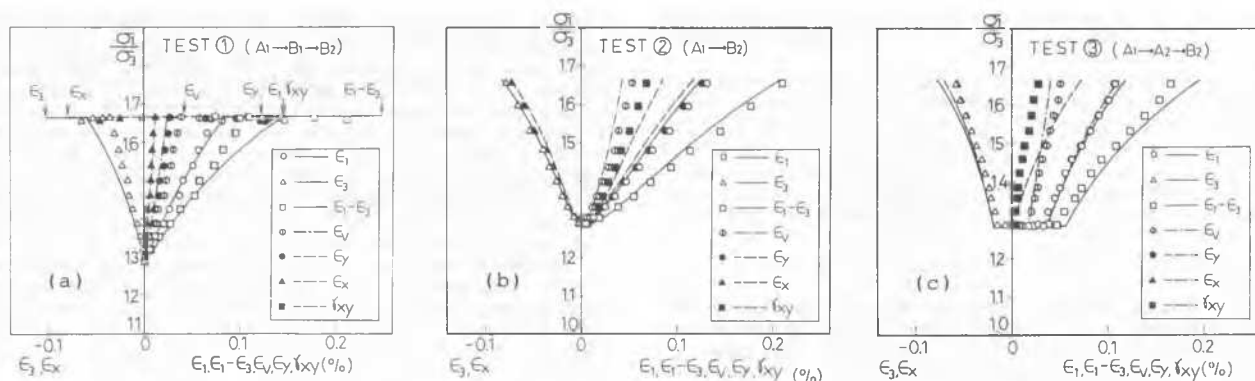


Fig. 7 Measured and Calculated Strains under Three Kinds of "General" Stress Paths ( $A_1 \rightarrow B_1 \rightarrow B_2$ ,  $A_1 \rightarrow B_2$  and  $A_1 \rightarrow A_2 \rightarrow B_2$ ) in Fig.6

time ( $A_1 \rightarrow B_2$  in Fig.6). Table I shows the final values of the principal strain  $\epsilon_1$  caused by the three kinds of "general" stress path tests. It is seen from Fig.7(a)-(c) that the values of strains are quite different along the three kinds of "general" stress paths, though the three kinds of "general" stress paths become the same in the  $\sigma_1$ - $\sigma_3$  diagram or the q-p diagram. It is seen from Table I that the final values of  $\epsilon_1$  are also different along the three kinds of "general" stress paths. This means that the "general" stress path dependency of strains is existent, because the starting point  $A_1$  and the final point  $B_2$  are the same for the three kinds of tests. The analytical values explain well such tendency of the measured values along the three kinds of "general" stress paths. The parameters used for all these analyses are as follows. For the stack of aluminium rods:  $\phi=24^\circ$ ,  $\lambda=0.8$ ,  $\mu=0.19$ ,  $k_s=0.31\%$  and  $\delta=30^\circ$ .

## CONCLUSIONS

The main results are summarized as follows:

- 1) A general stress apparatus which can apply the general stresses ( $\sigma_x$ ,  $\sigma_y$  and  $\tau_{xy}$ ) directly and independently has been made for a stack of aluminium rods as a two-dimensional model of granular materials. The general stresses  $\sigma_x$ ,  $\sigma_y$  and  $\tau_{xy}$  can be measured by load cells independently, and the general strains  $\epsilon_x$ ,  $\epsilon_y$  and  $\gamma_{xy}$  can be also measured by dial gauges independently.
- 2) A constitutive model for granular materials by which the general strain increments ( $d\epsilon_x$ ,  $d\epsilon_y$  and  $d\gamma_{xy}$ ) are directly related to the general stress increments ( $d\sigma_x$ ,  $d\sigma_y$  and  $d\tau_{xy}$ ) is proposed. The stress-strain matrix is expressed in general coordinates. The model predicts the strains not only due to "consolidation" and "shear", but also due to "principal stress rotation".
- 3) Using the general stress apparatus, "principal stress rotation tests" in which the stress state circles four times along a Mohr's stress circle are carried out to evaluate the influence of rotation of the principal stress axes on strains. The pretty large plastic strains are observed under the principal stress rotation with constant principal stresses, and they are analyzed by the proposed model.

Table I Measured and Calculated Final Principal Strain  $\epsilon_1$  under Three Kinds of "General" Stress Paths

	$\epsilon_1$ (%)	
	Measured	calculated
TEST ① ( $A_1 \rightarrow B_1 \rightarrow B_2$ )	0.15	0.15
TEST ② ( $A_1 \rightarrow B_2$ )	0.13	0.13
TEST ③ ( $A_1 \rightarrow A_2 \rightarrow B_2$ )	0.11	0.12

- 4) Using the same apparatus, three kinds of "general stress path tests" with the same starting and final stress points are also performed to investigate the general stress path dependency of strains. The observed strains are quite different along the three kinds of general stress paths, though the three kinds of general stress paths become the same in the  $\sigma_1$ - $\sigma_3$  diagram or the q-p diagram. All the test results are explained well by the proposed model.

## REFERENCES

- Matsuoka, H. (1974). Stress-strain relationships of sand based on the mobilized plane. *Soils and Foundations* (14), 2, 47-61.
- Matsuoka, H., Iwata, Y., and Sakakibara, K. (1986). A constitutive model of sands and clays for evaluating the influence of rotation of the principal stress axes. *Proc. 2nd Int. Symp. on Numerical Models in Geomechanics*, 67-78, Ghent.